Available online at www.sciencedirect.com
SCIENCE DIRECT®
Biochemical and Biophysical Research Communications 326 (2005) 799–804
BBRC
www.elsevier.com/locate/ybbrc

pH difference across the outer mitochondrial membrane measured with a green fluorescent protein mutant☆

Anna Maria Porcelli[a,*], Anna Ghelli[a], Claudia Zanna[a], Paolo Pinton[b], Rosario Rizzuto[b], Michela Rugolo[a]

[a] *Department of Biology, University of Bologna, Via Irnerio 42, 40126 Bologna, Italy*
[b] *Department of Experimental and Diagnostic Medicine, Section of General Pathology, Telethon Center for Cell Imaging (TCCI) and Interdisciplinary Center for the Study of Inflammation (ICSI), University of Ferrara, Via Borsari 46, 44100 Ferrara, Italy*

Received 9 November 2004
Available online 7 December 2004

Abstract

In this study we have generated a EYFP targeted to the mitochondrial intermembrane space (MIMS-EYFP) to determine for the first time the pH within this compartment. The fragment encoding HAI-tagged EYFP was fused with the C-terminus of glycerol-phosphate dehydrogenase, an integral protein of the inner mitochondrial membrane. Human ECV304 cells transiently transfected with MIMS-EYFP showed the typical mitochondrial network, co-localized with MitoTracker Red. Following the calibration procedure, an estimation of the pH value in the intermembrane space was obtained. This value (6.88 ± 0.09) was significantly lower than that determined in the cytosol after transfection with a cytosolic EYFP (7.59 ± 0.01). Further, the pH of the mitochondrial matrix, determined with a EYFP targeted to this subcompartment, was 0.9 pH units higher than that in the intermembrane space. In conclusion, MIMS-EYFP represents a novel powerful tool to monitor pH changes in the mitochondrial intermembrane space of live cells.

Keywords: Cytosolic pH; Mitochondria; Enhanced yellow fluorescent protein; ECV304 cells; Mitochondrial matrix pH; Mitochondrial intermembrane space pH

The renewed interest in mitochondria during recent years derives from recognition of their central role not only in cell energy production, but also in other important processes such as apoptosis and calcium homeostasis. It is widely accepted that the mitochondrial H^+ electrochemical potential ($\Delta\mu_{H^+}$), generated by electron transport across the inner membrane coupled to H^+ ejection through the redox H^+ pumps, is used to drive ATP synthesis by ATP-synthase. $\Delta\mu_{H^+}$ comprises both the electrical ($\Delta\Psi_m$) and the chemical components of the H^+ gradient (ΔpH). It is well established that under physiological conditions, $\Delta\Psi_m$ represents the dominant component of $\Delta\mu_{H^+}$, whereas the ΔpH gradient is small. The relative contribution of $\Delta\Psi_m$ and ΔpH across the mitochondrial inner membrane can be changed by redistribution of permeant ions such as phosphate, calcium or potassium, in the presence of the ionophore valinomycin.

Determination of $\Delta\Psi_m$ and ΔpH of mitochondria in intact cells is complex, due to the presence of the plasma membrane, with its own membrane potential and pH gradient. $\Delta\Psi_m$ can be monitored in situ with cationic fluorescent dyes that show specificity and sensitivity

☆ *Abbreviations:* BCECF, 2′,7′-bis(2-carboxyethyl)-5(6)carboxyfluorescein tetraacetoxy methyl ester; cyt-EYFP, cytosolic EYFP; EYFP, enhanced yellow fluorescent protein; GPD, glycerol-phosphate dehydrogenase; IMS, intermembrane space; MIMS-EYFP, EYFP targeted to mitochondrial intermembrane space; mt-EYFP, EYFP targeted to mitochondrial matrix; pH_i, intracellular pH; $\Delta\Psi_m$, mitochondrial membrane potential; ΔpH, pH gradient.

* Corresponding author. Fax: +39 051 242576.
E-mail address: porcelli@alma.unibo.it (A.M. Porcelli).

0006-291X/$ - see front matter © 2004 Elsevier Inc. All rights reserved.
doi:10.1016/j.bbrc.2004.11.105

[1]. Attempts carried out to measure matrix pH with conventional pH-sensitive dyes have been elusive, due to the difficulty in separating the mitochondrial signal from its surrounding cytoplasm [2].

One of the most promising tools developed to overcome this difficulty is represented by the use of recombinant pH-sensitive green fluorescent protein (GFP) mutants, which can be targeted to different intracellular compartments. The first of these GFP mutants targeted to the mitochondrial matrix of living cells was described in CHO cells [3]. However, expression of the recombinant GFP-mut1 did not allow accurate determination of the pH value of mitochondrial matrix because of its low pK_a [3]. Conversely, the expression of another pH-sensitive GFP mutant, named enhanced yellow fluorescent protein (EYFP), with the amino acid substitutions S65G/S72A/T203Y, and pK_a 7.1, allowed quantitative determination of changes of mitochondrial matrix pH in HeLa cells and rat neonatal cardiomyocytes. Indeed, the resting value (7.98 in HeLa cells and 7.91 in rat neonatal cardiomyocytes) rapidly collapsed to about pH 7 by protonophore addition, indicating that this GFP mutant provides a good tool for mitochondrial matrix pH measurements [4]. Other pH-sensitive GFP mutants were then developed, some of them also exhibiting spectral features suitable for ratiometric measurements [5–7].

While mitochondrial matrix pH can be monitored with the GFP mutants described above, the only measurement of pH in the intermembrane space (IMS) has been reported so far in intact mitochondria, after entrapping the fluorescent dye FITC–dextran in this compartment [8]. No measurements of pH in the IMS are available, however, in situ in intact cells. Historically, the outer membrane has not been considered a barrier to transport, due to the open configuration of the voltage-dependent anion channel (VDAC), a large diameter channel that is permeable to molecules up to 5 kDa [9,10]. Accordingly, it is generally assumed that the pH of this compartment is close to that of cytosol, although the hypothesis of a barrier to proton diffusion across the outer membrane has been proposed [8]. Moreover, IMS might be influenced by pH changes occurring in the matrix as a result of variations of mitochondrial volume or $\Delta\Psi_m$, and/or in cytosol by the presence of H^+ microdomains generated by other organelles, such as lysosomes/endosomes, or by the activity of plasma membrane H^+ transporters.

In this study, we have generated a EYFP targeted to IMS (MIMS-EYFP) to determine for the first time the pH within this mitochondrial compartment in intact cells. The choice of a GFP mutant with a pK_a value around 7 as a suitable pH sensor in this compartment derives from the assumption that the pH of IMS is close to that of cytosol. In addition, the pH value of the cytosol has been also determined with both cytosolic EYFP and the conventional pH-sensitive dye BCECF. The results presented demonstrate that in ECV304 cells the pH of the cytosol was remarkably different from that of the IMS.

Materials and methods

Materials. MitoTracker Red CMX-Ros and 2′,7′-bis(2-carboxyethyl)-5(6)carboxyfluorescein tetraacetoxy methylester (BCECF/AM) were purchased from Molecular Probes (Eugene, OR, USA); rotenone, oligomycin, monensin, and nigericin were from Sigma (St. Louis, MO, USA).

Construction of MIMS-EYFP. MIMS-EYFP has been constructed using the same cloning strategy employed for MIMS-aequorin [11]. Briefly, the *Cla*I/*Eco*RI fragment encoding HAI-tagged EYFP was generated by amplifying EYFP, using as template pEYFP-Tubulin (Clontech, Palo Alto, CA, USA) and primers Cla-F (5′-CC ATC GAT TAT GAT GTT CCT GAT TAT GCA AGC TTA ATG GTG AGC AAG GGC GAG GAG-3′) and *Eco*RI-R (5′-GAA TTC GAA TTC TTA CTT GTA CAG CTC GTC-3′). This fragment was inserted downstream of the internal *Cla*I site of the glycerol-phosphate dehydrogenase (GPD) cDNA and the recombinant protein was produced in *Escherichia coli* (MC1061). By this means, the two cDNAs were fused in-frame, and thus the encoded polypeptide includes aa 1–626 of GPD, the 9aa HAI tag, and EYFP.

Cell cultures and transient transfection. ECV304 cells were grown in M199 medium supplemented with 10% foetal bovine serum (FBS), 2 mM L-glutamine, 100 U/ml penicillin, and 100 μg/ml streptomycin. Cells were seeded on the glass coverslips (24 mm), grown to approximately 50–60% confluence, and then transiently transfected with 4 μg DNA plasmid of MIMS-EYFP, 8 μg DNA plasmid of cytosolic (cyt-EYFP) and of mitochondrial matrix-targeted EYFP (mt-EYFP), in which the mitochondrial presequence of subunit VIII of cytochrome *c* oxidase was fused to the EYFP cDNA. Cell transfection was carried out with the calcium-phosphate method [12].

Fluorescence microscopy. The imaging system was composed of an inverted epifluorescence microscope Nikon Eclipse 300 (Nikon Europe B.V., Badhoeverdorp, NL), with a back-illuminated CCD camera (Princeton Instruments, Trenton, NJ, USA) and acquisition/analysis software Metamorph/Metafluor (Universal Imaging, Downingtown, PA, USA), as described in [13]. Wavelength selection was accomplished using a dedicated YFP filter set (excitation, 488 ± 20 nm; emission, 500 ± 20 nm, Chroma Technologies, Brattleboro, VT, USA). The sensitivity of the camera results in reduction of the time of exposure to 50–100 ms. Under these conditions prolonged experiments can be carried out with a modest bleaching of the fluorophore (e.g., <20% in 5 min experiment with image acquisition at 1-to 2-s intervals). Cells were viewed with a 60× 1.4 oil immersion objective (Nikon).

pH determination. Experiments were performed 24–36 h after transfection. The coverslips with the cells were transferred to a perfusion chamber on the stage of the digital imaging system and perfused initially for 1–3 min with a Krebs-Ringer saline solution (KRS) containing: 125 mM NaCl, 5 mM KCl, 5.5 mM D-glucose, 1 mM $CaCl_2$, 1 mM $MgSO_4$, 1 mM K_2HPO_4, and 20 mM Na-Hepes (pH 7.4). Fluorescence images of single cell were acquired and regions of the interest were selected. Changes of fluorescence of these regions with time were determined by the acquisition/analysis software Metafluor. The perfusate was then switched to saline solutions with a K^+ concentration close to the cytosolic concentration (high K^+ saline solution), containing 125 mM KCl, 10 mM NaCl, 5.5 mM D-glucose, 1 mM $CaCl_2$, 1 mM $MgSO_4$, 1 mM K_2HPO_4, and 20 mM Na-Hepes, at pH 6.5, 7.0, 7.5, and 8.0, in the presence of the ionophores nigericin and monensin (5 μM) to equalize intracellular and extracellular pH. In some experiments, cytosol pH was also determined with the pH-sensitive dye BCECF/AM, as described in [14].

Mitochondrial morphology. Subcellular localization of MIMS-EYFP was determined after 24–36 h of transfection, followed by cell loading

with 10 nM MitoTracker Red, a specific mitochondrial dye, for 30 min at 37 °C. Mitochondrial morphology was observed with the digital imaging system described above.

Results and discussion

To obtain a direct measure of pH in IMS, we constructed a new EYFP chimera, denominated MIMS-EYFP. To this purpose, the cDNA encoding HAI-tagged EYFP was fused in-frame with encoding GPD [15], an integral protein of the inner mitochondrial membrane, with a large C-terminal tail protruding into the intermembrane space [16]. A schematic map of the final construct is shown in Fig. 1A. Based on the topology of GPD [16], the EYFP moiety is expected to be exposed in the mitochondrial intermembrane space, as illustrated in Fig. 1B. ECV304 cells transiently transfected with MIMS-EYFP exhibited the typical mitochondrial pattern diffuse in the cytosol and around the nucleus (Fig. 1C, panel a) [17,18]. Analysis of the same cells stained with MitoTracker Red, a specific mitochondrial dye, showed a clear co-localization with MIMS-EYFP pattern (Fig. 1C, panels b and c).

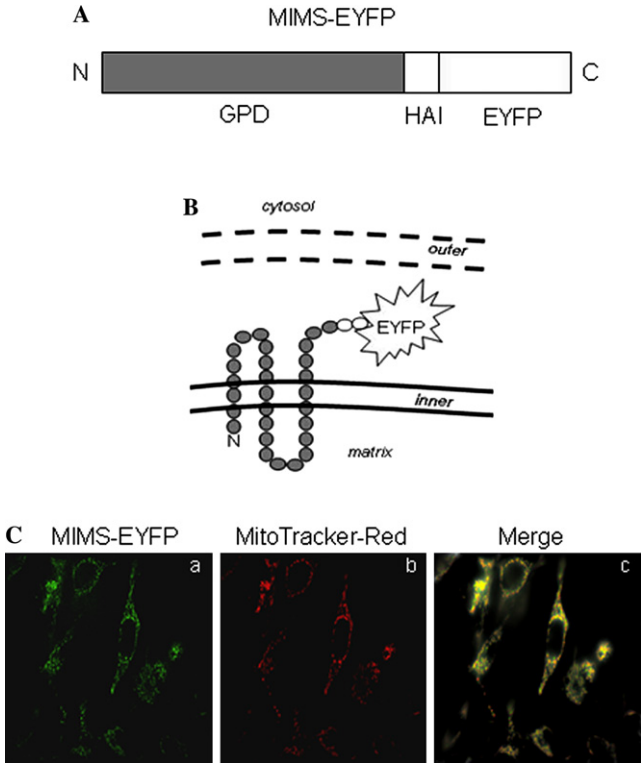

Fig. 1. MIMS-EYFP: structure and mitochondrial localization. (A) Schematic map of the MIMS-EYFP cDNA, where regions encoding aa 1–626 of GPD, HAI epitope (HAI), and EYFP are shown. (B) Putative submitochondrial localization of MIMS-EYFP. (C) Fluorescence images of living ECV304 cells transfected with MIMS-EYFP (panel a), then incubated for 30 min with 10 nM MitoTracker Red (panel b), and merge of the two images (panel c). The two probes were selectively excited at 480 nm (panel a) and 602 nm (panel b). Cells were transfected and observed with a 40× objective, using a digital imaging analysis system described in Materials and methods.

Quantitative determination of MIMS-EYFP fluorescence signal was then carried out in selected areas of cells (average 5–6 areas per cell). The incubation medium was then switched to a high K^+ saline solution, containing 5 μM nigericin and 5 μM monensin, which equilibrate intra- and extracellular pH. Perfusion with saline solutions at the indicated pH allowed the construction of the titration curve shown in Fig. 2A. When the average values of fluorescence in the selected areas were plotted against pH, the calibration line shown in Fig. 2B was obtained. A similar calibration was carried out also in cells transfected with cyt-EYFP and with mt-EYFP (data not shown). With this calibration, the pH values obtained were 6.88 ± 0.09 ($n = 32$) in the IMS, 7.78 ± 0.17 ($n = 9$) in the matrix, and 7.59 ± 0.01 ($n = 21$) in the cytosol, as illustrated in Fig. 3. Although during our experiments the chloride concentration was kept constant, we noticed that fluorescence values at different pHs were not influenced by replacement of chloride in the medium by gluconate, indicating that, in contrast to other GFP mutants [19], MIMS-EYFP is poorly halide sensitive (result not shown).

The cytosol pH value obtained with EYFP is very similar to that determined from experiments with the pH-sensitive dye BCECF (7.51 ± 0.15, $n = 5$). These pH values are significantly higher than those previously reported by us in ECV304 cells incubated in bicarbonate-buffered

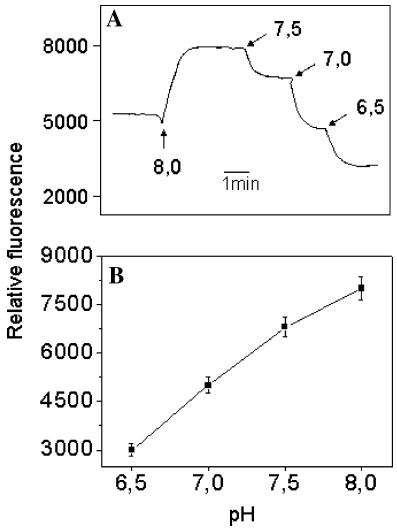

Fig. 2. In situ titration of fluorescence versus pH in ECV304 cells expressing MIMS-EYFP. (A) A representative trace of fluorescence changes of MIMS-EYFP-transfected ECV304 cells incubated with KRS and then perfused with high K^+ saline solution containing nigericin and monensin (5 μM) at the indicated pH is shown (see Materials and methods for details). (B) Normalized values of fluorescence intensity, obtained as described in (A), were plotted against the pH values of solution. The linear regression coefficient was between 0.95 and 0.97 ($n = 30$). Data are means ± SD of 30 determinations.

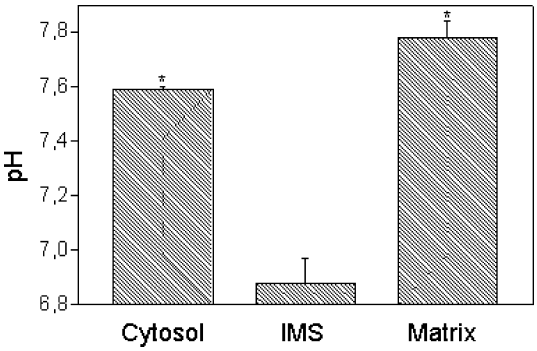

Fig. 3. Values of pH in the cytosol, IMS, and mitochondrial matrix of ECV304 cells. ECV304 cells were transfected with cyt-EYFP or MIMS-EYFP or mt-EYFP, incubated with KRS, and then calibration of fluorescence intensity was carried out as described in Fig. 2. Values are means ± SD of 21, 9, and 32 determinations, respectively. The asterisk denotes values significantly different from the pH value of IMS ($P < 0.001$).

saline solution and kept under 95% air and 5% CO_2 atmosphere (7.29 ± 0.04, $n = 3$) [14]. We have previously shown in other cellular systems that in bicarbonate-buffered media, pH_i was about 0.3–0.4 pH unit lower than in Hepes-buffered media [20].

The response of MIMS-EYFP fluorescence to changes of IMS pH in vivo was first determined by addition of 20 mM NH_4Cl, which caused a rapid rise in fluorescence, due to alkalinization caused by NH_3 transport and NH_3/NH_4^+ equilibration (Fig. 4A). After perfusion without NH_4Cl, a prompt acidification was observed, clearly indicating that MIMS-EYFP fluorescence responded rapidly to pH changes. Furthermore, pre-incubation with rotenone (2 μM) plus oligomycin (2 μg/ml), inhibitors of complex I and ATP synthase, respectively, also induced a significant alkalinization (Fig. 4B). This result indicates that pH of IMS is significantly influenced by the respiratory chain function.

One important novel finding of this study is that the pH value of the IMS is significantly lower than that of the cytosol. Taking into consideration the model of the internal structure of mitochondria recently proposed [21], it is apparent that the connection between cristae and the IMS is limited in extent due to the presence of cristae junctions with restricted diameter. Cristae junctions thus might restrict diffusion of integral membrane proteins, creating functional compartments of inner membrane between the inner boundary membrane and the cristae membrane [21]. In this regard, it has been shown that both the respiratory complexes and ATP synthase are preferentially localized in the cristae, which therefore represent a subcompartment of the inner membrane specialized for oxidative phosphorylation [22,23]. If the MIMS-EYFP is also mainly localized in the cristae compartment and only to a very low extent in the inner membrane subcompartment facing the outer mitochondrial membrane, it would therefore be more influ-

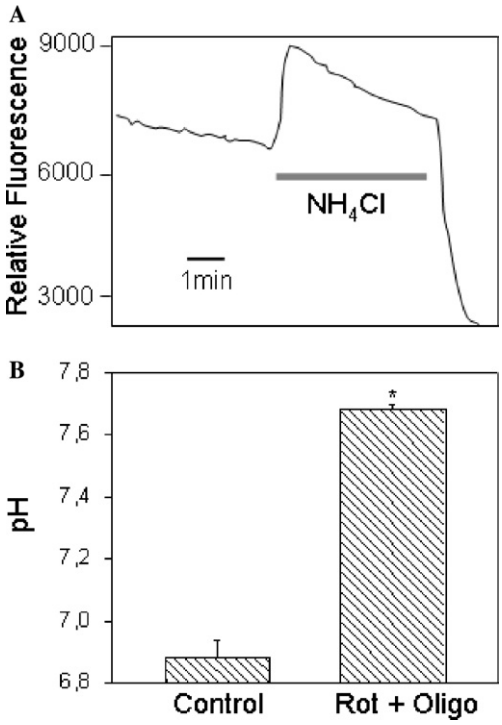

Fig. 4. Effect of NH_4Cl and mitochondrial inhibitors in ECV304 cells transfected with MIMS-EYFP. (A) MIMS-EYFP-transfected ECV304 cells were incubated in KRS and then perfused with the same solution containing 30 mM NH_4Cl for the time indicated by the grey line. The experiment is representative of three similar ones. (B) MIMS-EYFP-transfected ECV304 cells were incubated in KRS in the absence or presence of 2 μM rotenone and 2 μg/ml oligomycin, and then calibration of fluorescence intensity was carried out as described in Fig. 2. Data are means ± SD of six determinations. The asterisk denotes a value significantly different from untreated cells (control, $P < 0.001$).

enced by H^+ release from the respiratory complexes within the cristae than by H^+ changes occurring in the cytosol. The results presented here are in agreement with those previously reported in isolated mitochondria, showing that the IMS pH was 0.4–0.5 lower than the bulk pH in the incubation medium [8].

Due to the presence of VDAC, it is highly likely that the protons are at electrochemical equilibrium in the compartments separated by the outer membrane, also in the presence of a remarkable pH difference. The ΔpH and $\Delta\Psi_m$ might indeed act in opposite directions to achieve a Donnan electrochemical equilibrium. The existence of a equilibrium potential across the outer membrane of mitochondria was proposed years ago by Colombini [9] due to the VDAC location in this membrane. Indeed, the presence of different charged macromolecules, mainly proteins, in the cytosol and IMS requires that a Donnan potential be established across the outer membrane. An important implication of our results is that it is possible for the first time to provide an estimation of this potential, from the $[H^+]$ values in the two compartments by means of the Nernst equation.

Interestingly, a value of 43 mV was obtained, which is very similar to the voltage required in electrophysiological experiments to switch the conductance of VDAC incorporated in a planar membrane from a high to a low conductance (15–40 mV) [9].

The second relevant finding reported in this study is the assessment of a significant pH difference between the compartments delimited by the inner mitochondrial membrane. A pH difference was obviously expected according to the chemiosmotic theory predictions. The magnitude of the mitochondrial proton electrochemical potential across the inner membrane in isolated rat liver mitochondria was 200–220 mV. In particular, the $\Delta\Psi_m$ component, determined by tetraphenylphosphonium distribution, was close to 170 mV, whereas the ΔpH contribution, assessed by the weak acid acetate distribution, was $\leqslant$0.5 ΔpH units [1]. The ΔpH value measured in this study between the two compartments is therefore remarkably higher than expected on the basis of the isolated mitochondria measurements. On the other hand, it is possible that the value of $\Delta\Psi_m$ in situ is lower than that of isolated mitochondria. Unfortunately, this specific issue is difficult to assess, since methods for determination of $\Delta\Psi_m$ in intact cells provide only a qualitative evaluation [24]. In vivo, mitochondrial depolarization might also be the result of the uptake of cations, calcium for instance, leading to compensatory increase of ΔpH. Finally, we cannot exclude a priori that the pH values obtained from EYFP measurements might be influenced by the cell type and/or metabolism (glycolytic versus oxidative). In this regard, studies of overexpression of mitochondrial targeted EYFPs in other cell lines and primary cultures are in progress (to be reported elsewhere).

In spite of the above-illustrated considerations, it is apparent that MIMS-EYFP represents a powerful tool that allows for the first time to monitor pH changes in the mitochondrial IMS of intact live cells. This new probe has the great advantage to be specifically targeted to this mitochondrial compartment, where many important proteins involved in cell function regulation are localized. Furthermore, the stability of this protein and the lack of toxicity make it ideal indicator for a wide array of cellular applications in vivo. It will be possible to assess whether some regions of mitochondria are more active than others in H^+ translocation and whether pH changes occur in the IMS after activation of cell surface receptors or during the onset of apoptosis.

Acknowledgments

This work was supported by grants from the University of Bologna ''Progetto Dipartimentale: Meccanismi e segnali molecolari della sopravvivenza cellulare'' to M.R., Telethon, Italy No. GGP02323 to A.G., No. 1285 and GTF02013 to R.R., the Italian Association for Cancer Research (AIRC), the Human Frontier Science Program, the Italian University Ministry (MIUR and FIRB), and the Italian Space Agency (ASI) to R.R. We are grateful to Dr. G. Venturoli, University of Bologna, for critical reading of the manuscript.

References

[1] D.G. Nicholls, S.F. Fergusson, Quantitative bioenergetics: the measurements of driving forces, in: Bioenergetics 2, Academic Press, London, 1992, pp. 39–63.
[2] E. Chacon, J.M. Reece, A. Nieminen, G. Zahrebelski, B. Herman, J.J. Lemasters, Distribution of electrical potential, pH, free Ca^{2+}, and volume inside cultured adult rabbit cardiac myocytes during chemical hypoxia: a multiparameter digitized confocal microscopic study, Biophys. J. 66 (1994) 942–952.
[3] M. Kneen, J. Farinas, Y. Li, A.S. Verkman, Green fluorescent protein as a noninvasive intracellular pH indicator, Biophys. J. 74 (1998) 1591–1599.
[4] J. Llopis, J.M. McCaffery, A. Miyawaki, M. Farquhar, R.Y. Tsien, Measurement of cytosolic, mitochondrial, and Golgi pH in single living cells with green fluorescent proteins, Proc. Natl. Acad. Sci. USA 95 (1998) 6803–6808.
[5] M.A. Elsliger, R.M. Wachter, G.T. Hanson, K. Kallio, S.J. Remington, Structural and spectral response of green fluorescent protein variants to changes in pH, Biochemistry 38 (1999) 5296–5301.
[6] R. Rossignol, R. Gilkerson, R. Aggeler, K. Yamagata, S.J. Remington, R.A. Capaldi, Energy substrate modulates mitochondrial structure and oxidative capacity in cancer cells, Cancer Res. 64 (2004) 985–993.
[7] M.F. Cano Abad, G. Di Benedetto, P.J. Magalhães, L. Filippin, T. Pozzan, Mitochondrial pH monitoring by a new engineered GFP mutant, J. Biol. Chem. 279 (2004) 11521–11529.
[8] J.D. Cortese, A.L. Voglino, C.R. Hackenbrock, The ionic strength of the intermembrane space of intact mitochondria is not affected by the pH or volume of the intermembrane space, Biochim. Biophys. Acta 1100 (1992) 189–197.
[9] M. Colombini, A candidate for the permeability pathway of the outer mitochondrial membrane, Nature 279 (1979) 643–645.
[10] C. Mannella, W.D. Bonner, X-ray diffraction from oriented outer mitochondrial membranes. Detection of in-plane subunit structure, Biochim. Biophys. Acta 413 (1975) 226P–233P.
[11] P. Pinton, M. Brini, C. Bastianutto, R.A. Tuft, T. Pozzan, R. Rizzuto, New light on mitochondrial calcium, BioFactors 8 (1998) 243–253.
[12] R. Rizzuto, M. Brini, C. Bastianutto, R. Marsault, T. Pozzan, Photoprotein-mediated measurement of calcium ion concentration in mitochondria of living cells, Methods Enzymol. 260 (1995) 417–428.
[13] R. Rizzuto, W. Carrington, R.A. Tuft, Digital imaging microscopy of living cells, Trends Cell Biol. 8 (1998) 288–292.
[14] A. Ghelli, A.M. Porcelli, C. Zanna, M. Rugolo, 7-Ketocholesterol and staurosporine induce opposite changes in intracellular pH associated with distinct types of cell death in ECV304 cells, Arch. Biochem. Biophys. 402 (2002) 208–217.
[15] L.J. Brown, M.J. MacDonald, D.A. Lehn, S.M. Moran, Sequence of rat mitochondrial glycerol-3-phosphate dehydrogenase cDNA. Evidence for EF-hand calcium-binding domain, J. Biol. Chem. 269 (1994) 14363–14366.
[16] M.J. MacDonald, L.J. Brown, Calcium activation of mitochondrial glycerol phosphate dehydrogenase restudied, Arch. Biochem. Biophys. 326 (1996) 79–84.

[17] T.J. Collins, M.J. Berridge, P. Lipp, M.D. Bootman, Mitochondria are morphologically and functionally heterogeneous within cells, EMBO J. 21 (2002) 1616–1627.
[18] A.M. Porcelli, P. Pinton, E.K. Ainscow, A. Chiesa, M. Rugolo, G.A. Rutter, R. Rizzuto, Targeting of reporter molecules to mitochondria to measure calcium. ATP and pH, Methods Cell Biol. 65 (2001) 353–380.
[19] R.M. Wachter, S.G. Remington, Sensitivity of the yellow variant of green fluorescent protein to halides and nitrate, Curr. Biol. 9 (1999) R628–R629.
[20] A.M. Porcelli, K. Scotlandi, S. Strammiello, G. Gislimberti, N. Baldini, M. Rugolo, Intracellular pH regulation in U-2 OS human osteosarcoma cells transfected with P-glycoprotein, Biochim. Biophys. Acta 1542 (2002) 125G–130G.
[21] T.G. Frey, C.A. Mannella, The internal structure of mitochondria, Trends Biochem. Sci. 25 (2000) 319–324.
[22] Y.H. Ko, M. Delannoy, J. Hullihen, W. Chiu, P.L. Pedersen, Mitochondrial ATP synthasome. Cristae-enriched membranes and a multiwell detergent screening assay yield dispersed single complexes containing the ATP synthase and carriers for Pi and ADP/ATP, J. Biol. Chem. 278 (2003) 12305–12309.
[23] R.W. Gilkerson, J.M. Selker, R.A. Capaldi, The cristal membrane of mitochondria in the principal size of oxidative phosphorylation, FEBS Lett. 546 (2003) 355–358.
[24] D.G. Nicholls, M.W. Ward, Mitochondrial membrane potential and neuronal glutamate excitotoxicity: mortality and millivolts, Trends Neurosci. 23 (2000) 166–174.